Chinese Chemical Letters 33 (2022) 4545–4548

Contents lists available at ScienceDirect

Chinese Chemical Letters

journal homepage: www.elsevier.com/locate/cclet

Nitrogen-bridged Ni(II) porphyrinoid trimers with a central quinodiimine unit

Kaisheng Wang[a], Boyu Xiao[a], Ling Xu[a], Mingbo Zhou[a], Takayuki Tanaka[b], Atsuhiro Osuka[a], Jianxin Song[a,*]

[a] College of Chemistry and Chemical Engineering, Key Laboratory of Chemical Biology and Traditional Chinese Medicine Research (Ministry of Education of China), Key Laboratory of the Assembly and Application of Organic Functional Molecules of Hunan Province, Hunan Normal University, Changsha 410081, China

[b] Department of Chemistry, Graduate School of Science Kyoto University, Kyoto 606-8502, Japan

ARTICLE INFO

Article history:
Received 18 November 2021
Revised 18 January 2022
Accepted 23 January 2022
Available online 31 January 2022

Keywords:
Porphyrinoid trimer
Aminoporphyrins
Buchwald-Hartwig amination
Reduction
Charge transfer

ABSTRACT

Buchwald-Hartwig amination of 5,15-dibromo and 5,10-dibromo Ni(II)porphyrins with 5-amino Ni(II)porphyrin gave linear and bent trimers **4Ni** and **5Ni** with a central quinodiimine-type Ni(II)porphyrinoid. The structures of **4Ni** and **5Ni** have been confirmed by X-ray diffraction analysis in both cases. The formation of unusual products **4Ni** and **5Ni** has been ascribed to facile oxidation of 5,15- and 5,10-amino Ni(II) porphyrin unit. Reduction of **4Ni** and **5Ni** under proper conditions gave NH-bridged Ni(II)porphyrin trimers **4Ni-2H** and **5Ni-2H** in high yields. Trimers **4Ni** and **5Ni** exhibit the lowest energy band as compared with **4Ni-2H** and **5Ni-2H**. Especially the bent trimer **5Ni** exhibits a broad absorption tail beyond 1400 nm.

Porphyrin arrays are organic functional molecules with large π-conjugated systems and have potential applications in optoelectronic devices [1–11], sensors [12–15] and photodynamic therapy (PDT) [16–18]. In the last decade, porphyrin arrays with alkynes [19,20], benzene [21] or heterocycles (such as thiophene [22], pyridine [23], pyrrole [24,25]) as bridging units have been intensively studied. Porphyrin dimers with a single carbon or heteroatom bridging unit have received much attention due to their unique photophysical properties, chemical properties, and characteristic electronic delocalization [26–37]. In 2006, Arnold *et al.* reported the first isolation of *meso–meso* nitrogen-bridged diporphyrinylamine **1**, which showed a broadened Soret band and red shift Q bands, indicating substantial electronic interaction between the porphyrins [27]. Ruppert *et al.* reported *meso–meso*, *β–meso*, *β-β*-nitrogen-bridged diporphyrinylamines [29], which were all synthesized by Buchwald-Hartwig amination. Later, Osuka *et al.* reported that *meso–meso* nitrogen-bridged Ni(II) porphyrin dimer was cleanly converted into aminyl radical **2** and nitrenium cation **3** by oxidation with PbO_2 and tris(4-bromophenyl)aminiumyl hexachloroantimonate (Magic Blue), respectively (Fig. 1) [34]. As an extension, we report here the synthesis of nitrogen-atom bridged Ni(II) porphyrin trimers.

First we attempted to synthesize linear NH-bridged porphyrin trimer **4Ni-2H** by the similar Buchwald-Hartwig amination of 5,15-dibromo Ni(II)porphyrin **7Ni** with 5-amino Ni(II)porphyrin **6Ni** [34]. A 4:1 solution of **6Ni** and **7Ni** in toluene was heated at 100 °C for 12 h in the presence of 0.4 equiv. $Pd(OAc)_2$, 0.4 equiv. BINAP, and 7 equiv. *t*-BuOK (Scheme 1). To our surprise, only a linear trimer **4Ni** bearing a central quinodiimine-type porphyrinoid unit was obtained in 38% yield. The matrix-assisted laser desorption ionization time-of-flight (MALDI-TOF) mass spectrum showed the parent ion of **4Ni** at *m/z* 2627.3453 $[M]^+$ (calcd. for $(C_{172}H_{192}N_{14}Ni_3)^+ = 2627.3509$) (Fig. S13 in Supporting information), which is smaller by two than the expected parent ion peak of **4Ni-2H**. The structure of **4Ni** has been revealed by X-ray diffraction structural analysis (Fig. 2 and Fig. S17 in Supporting information). The bond lengths of $C2_{meso}$-N (1.300(6) Å and 1.304(6) Å) are distinctly shorter than those of $C1_{meso}$-N (1.412(6) Å and 1.395(7) Å). The ^{1}H NMR spectrum of **4Ni** showed broadened signals at room temperature in $CDCl_3$ (Fig. S3 in Supporting information), which gradually changed to sharp peaks upon cooling down to −60 °C (Fig. S4 in Supporting information) [38], suggesting conformational motions at room temperature, which are comparable or faster than ^{1}H NMR timescale. It is noteworthy that four doublets due to the *b*-protons of the central quinodiimine unit were observed in the up-field shifted region at 7.77, 6.76, 5.70 and 3.99 ppm.

* Corresponding author.
E-mail address: jxsong@hunnu.edu.cn (J. Song).

https://doi.org/10.1016/j.cclet.2022.01.061
1001-8417/

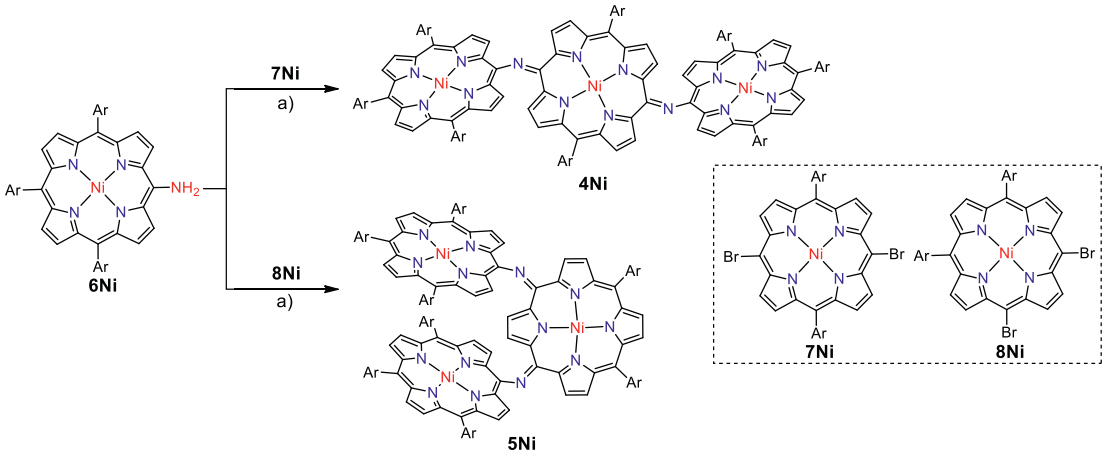

Scheme 1. Syntheses of *meso*–*meso* *N*-bridged porphyrinoid trimers. Conditions: a) $Pd(OAc)_2$, BINAP, *t*-BuOK, toluene, 100 °C, 12 h. Ar = 3,5-di–*tert*-butylphenyl.

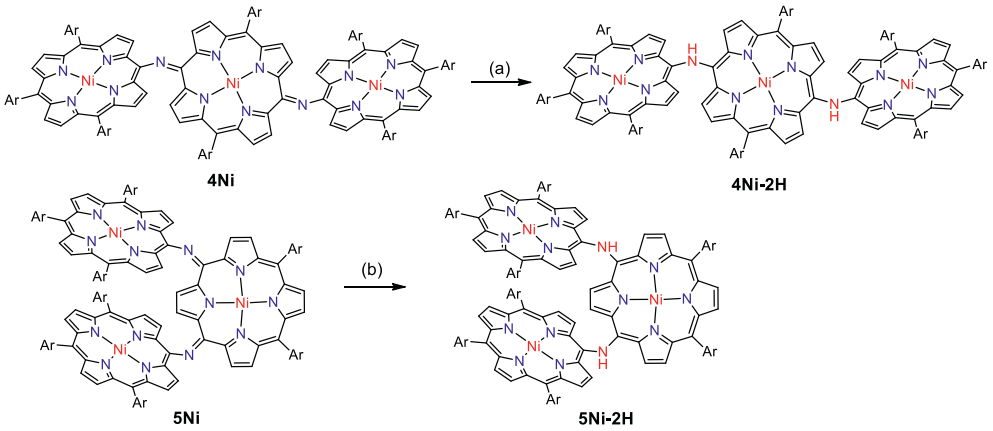

Scheme 2. Syntheses of *meso*–*meso* NH-bridged porphyrin trimers. Conditions: (a) $NaBH_4$, Pd/C, CH_2Cl_2/CH_3OH; (b) $NH_2–NH_2·H_2O$, CH_2Cl_2. Ar = 3,5-di–*tert*-butylphenyl.

Similarly, Buchwald-Hartwig amination of 5,10-dibromo Ni(II)porphyrin **8Ni** with **6Ni** afforded L-shaped bent trimer **5Ni** in 25% yield. The quinodiimine structure of **5Ni** has been also confirmed by X-ray analysis. **5Ni** shows that the bond lengths of C2$_{meso}$-N (1.299(5) Å and 1.302(6) Å) are shorter than those of C1$_{meso}$-N bonds (1.399(5) Å and 1.413(6) Å) (Fig. 2 and Fig. S18 in Supporting information). The ^{1}H NMR spectrum of **5Ni** showed broadened signals at room temperature that became sharp and complicated signals at −60 °C in $CDCl_3$ (Figs. S5 and S6 in Supporting information). In line with the quinodiimine structure, the corresponding β-protons were observed in the high field at 7.07, 6.73, 6.42, 6.33, 5.66, 4.33, and 3.74 ppm.

The structural data of **4Ni** shows that lengths of C1$_{meso}$-N bonds (1.412(6) Å and 1.395(7) Å) bond to the terminal porphyrin units are longer than C2$_{meso}$-N (1.300(6) Å and 1.304(6) Å) attached to the central quinodiimine units. Similarly, **5Ni** shows that lengths of C1$_{meso}$-N bonds (1.399(5) Å and 1.413(6) Å) bond to the terminal porphyrin units are longer than C2$_{meso}$-N (1.299(5) Å and 1.302(6) Å) attached to the central quinodiimine units. The observed short C2$_{meso}$-N bond lengths in **4Ni** and **5Ni** indicated its double bond characters significantly [34], which further proved the structure of **4Ni** and **5Ni** to be *N*-bridged (rather than NH-bridged) porphyrin trimer. The dihedral angles between the terminal porphyrins and terminal porphyrin, terminal porphyrin and central quinodiimine are 66.81(3)°, 56.34(3)° and 58.06(3)° in **4Ni**, and 6.83(3)°, 42.67(3)° and 39.34(3)° in **5Ni** (Fig. 2 and Figs. S17 and S18 in Supporting information).

Electrochemical properties of **4Ni** and **5Ni** were examined by cyclic voltammetry and differential-pulse voltammetry in CH_2Cl_2 against a ferrocene/ferrocenium ion couple (Table 1 and Table S4 in Supporting information). Reversible oxidation waves were recorded at 0.22 and 0.52 V for **4Ni**, and at 0.12 and 0.23 V for **5Ni**. Reversible reduction waves were observed at −1.02 and −1.11 V for **4Ni**, and at −0.79 and −1.14 V for **5Ni** (Figs. S20 and S21 in Supporting information). As a result, the electrochemical HOMO-LUMO gaps of **4Ni** and **5Ni** were determined to be 1.24 and 0.91 eV, respectively. The observed reversible reduction waves of **4Ni** and **5Ni** encouraged us to examine their chemical reduction. After many attempts, we found that reduction of **5Ni** with aqueous hydrazine in CH_2Cl_2 afforded **5Ni-2H** quantitatively (Scheme 2). Curiously, **4Ni** was not reduced with aqueous hydrazine but was reduced quantitatively to give **4Ni-2H** with $NaBH_4$ and Pd/C in CH_2Cl_2/CH_3OH. ^{1}H NMR spectra of both **4Ni-2H** and **5Ni-2H** are very simple, reflecting their symmetric structures with signals of the β-protons appearing in the range of 8–9 ppm (Fig. 3 and Figs. S7 and S8 in Supporting information). The structure of **5Ni-2H** has been confirmed by single crystal X-ray diffraction analysis (Fig. 4 and Fig. S19 in Supporting information). In **5Ni-2H**, the bond lengths of the C2$_{meso}$-N bond and the C1$_{meso}$-N bond are similar, being 1.409(8) Å, 1.406(8) Å and 1.393(7) Å, 1.434(11) Å, respectively, in line with the assigned structures. In addition, the dihedral angles between the terminal porphyrins and the central porphyrin are 58.29(7)° and 58.15(7)°, which are larger than those on **5Ni** (42.67(3)° and 39.34(3)°).

Table 1
Electrochemical measurement of **4Ni, 5Ni, 4Ni-2H** and **5Ni-2H** performed in CH_2Cl_2 at room temperature.[a]

Compound	E_{ox3} (V)	E_{ox2} (V)	E_{ox1} (V)	E_{red1} (V)	E_{red2} (V)	E_{HL} (eV)[b]
4Ni		0.52	0.22	−1.02	−1.11	1.24
5Ni		0.23	0.12	−0.79	−1.14	0.91
4Ni-2H		0.17	−0.09	−1.92		1.83
4Ni-2H	0.41	0.25	0.11	−1.79		1.90

[a] Potentials (V) *vs.* ferrocene/ferrocenium ion. Scan rate 0.05 V/s; working electrode, glassy carbon; counter electrode, Pt wire; supporting electrolyte, 0.1 mol/L nBu$_4$NPF$_6$ in CH_2Cl_2; reference electrode, Ag/AgNO$_3$.
[b] Electrochemical HOMO-LUMO gaps (ΔE_{HL} = e($E_{ox.1}$-$E_{red.1}$) (eV)).

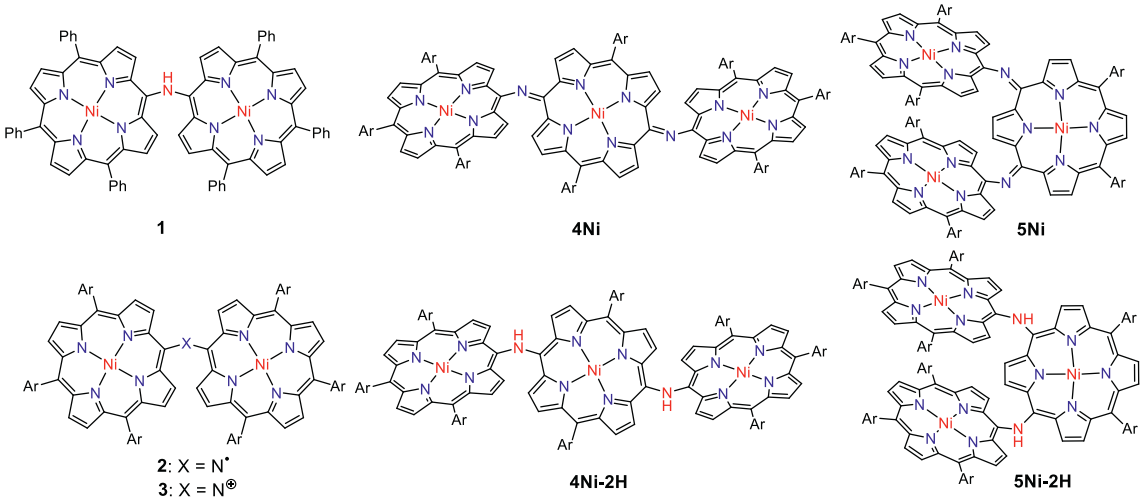

Fig. 1. *N*-Bridged porphyrin oligomers. Ar = 3,5-di–*tert*-butylphenyl.

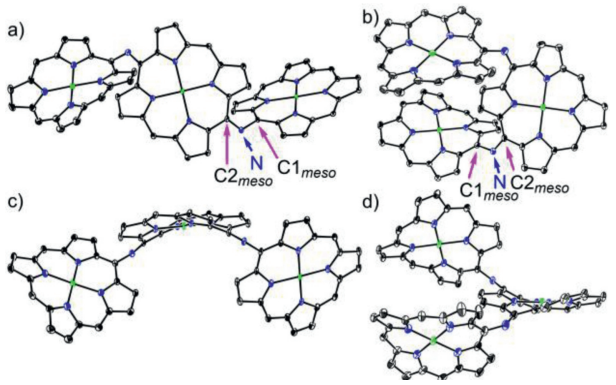

Fig. 2. X-ray single crystal structure of **4Ni** and **5Ni**. (a) Top view and (b) side view of **4Ni**, (c) top view and d) side view of **5Ni**. The thermal ellipsoids are on 30% probability level. Solvent molecules, 3,5-di–*tert*-butylphenyl groups, and hydrogens are omitted for clarity.

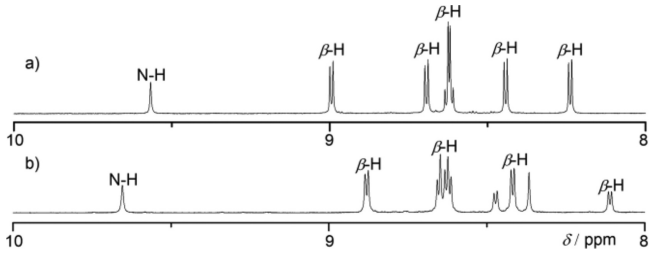

Fig. 3. Partial ^{1}H NMR spectra of (a) **4Ni-2H** and (b) **5Ni-2H**.

The unexpected formation of **4Ni** and **5Ni** may be ascribed to the facile oxidation of **4Ni-2H** and **5Ni-2H** under the amination reaction conditions. These trimers have the central electron-rich

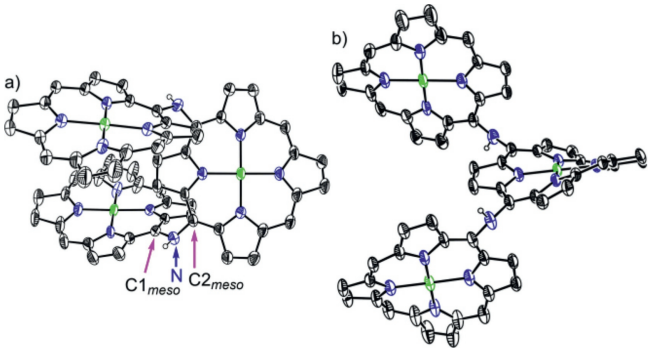

Fig. 4. X-ray single crystal structure of **5Ni-2H**. (a) Top view and (b) side view. The thermal ellipsoids are on 30% probability level. Solvent molecules, 3,5-di–*tert*-butylphenyl groups, and hydrogens except those connected to N atoms are omitted for clarity.

Ni(II) porphyrin bearing 5,15 or 5,10-aminoporphyrin units. Thus, we examined the electrochemical properties of **4Ni-2H** and **5Ni-2H** (Table 1 and Table S4 in Supporting information). Actually, the reversible oxidation waves were observed at −0.09 and 0.17 V for **4Ni-2H**, and at 0.11, 0.25 and 0.41 V for **5Ni-2H** (Figs. S22 and S23 in Supporting information). It is thus conceivable that **4Ni-2H** and **5Ni-2H** are oxidized under the amination conditions with air. So, when we try to oxidized them with PbO_2 and Magic Blue, neither aminyl radical nor nitrenium cation was found. The possible reason may be that the quinodiimine unit is more stable than other species.

The UV–vis-NIR absorption spectra of **4Ni, 5Ni, 4Ni-2H** and **5Ni-2H** in CH_2Cl_2 are shown in Fig. 5. **4Ni** shows two split Soret bands at 426 and 472 nm, a Q-band at 537 nm, and a broadened Q-like band at 915 nm. **5Ni** shows a Soret band at 429 nm,

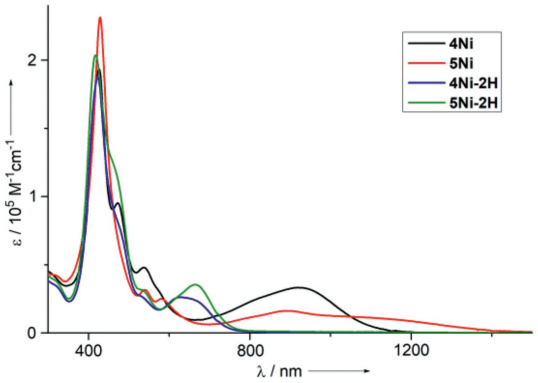

Fig. 5. UV–vis-NIR absorption spectra of **4Ni** (black line), **5Ni** (red line), **4Ni-2H** (blue line) and **5Ni-2H** (green line) in CH_2Cl_2.

Q-bands at 540 and 581 nm, and a broadened Q-like band at 892 nm. Both **4Ni** and **5Ni** exhibit characteristic absorption spectra of quinonoidal porphyrinoid arrays [39–42]. **4Ni-2H** shows a Soret band at 423 nm, and a Q-band at 627 nm. Similarly to **4Ni-2H**, the absorption spectrum of **5Ni-2H** shows a Soret band at 418 nm, and a Q-band at 664 nm. In particular, **4Ni** and **5Ni** display the lowest energy band reaching to 1200 nm and 1400 nm, respectively.

Density functional theory (DFT) calculations clearly indicated that both the HOMO of **4Ni** and HOMO-1 **5Ni** were localized at terminal porphyrin units, whereas both LUMOs of **4Ni** and **5Ni** were localized at the central quinodiimine units (Figs. S28 and S29 in Supporting information). Time-dependent density functional theory (TD-DFT) calculations indicated that the absorption bands around 1000 nm of trimers **4Ni** and **5Ni** resulted from the transition from HOMO to LUMO of **4Ni** and HOMO-1 to LUMO of **5Ni**, respectively (Figs. S24 and S25 in Supporting information). These results show that both absorption bands around 1000 nm of **4Ni** and **5Ni** could be assigned to charge transfer (CT) band.

In summary, we synthesized *N*-bridged porphyrinoid trimers **4Ni** and **5Ni** having the central quinodiimine through Buchwald-Hartwig amination, under which the oxidations of the NH-bridged porphyrin trimers **4Ni-2H** and **5Ni-2H** proceeded smoothly. The trimer **4Ni-2H** was obtained by reduction with $NaBH_4$ and Pd/C, while **5Ni-2H** was obtained by reduction with aqueous hydrazine. The structures of **4Ni, 5Ni** and **5Ni-2H** were determined by X-ray diffraction analysis. The UV–vis-NIR absorption spectra showed that the trimers **4Ni** and **5Ni** have the lowest energy band reaching to 1200 nm and 1400 nm, respectively. These *N*-bridged porphyrinoid trimers exhibited interesting spectral properties. Further exploration of cyclic or larger *N*-bridged porphyrinoid arrays is ongoing in our laboratory.

Declaration of competing interest

The authors declare that they have no known competing financial interests or personal relationships that could have appeared to influence the work reported in this paper.

Acknowledgments

The work at Hunan Normal University was supported by the National Natural Science Foundation of China (Nos. 21772036, 22071052, 21602058, 21702057), the Science and Technology Planning Project of Hunan Province (No. 2018TP1017), and the Scientific Research Fund of Hunan Provincial Education Department (No. 19A331), and Hunan Provincial Innovation Foundation for Postgraduate (No. CX20210473).

Supplementary materials

Supplementary material associated with this article can be found, in the online version, at doi:10.1016/j.cclet.2022.01.061.

References

[1] A. Tsuda, A. Osuka, Science 293 (2001) 79–82.
[2] D. Holten, D.F. Bocian, J.S. Lindsey, Acc. Chem. Res. 35 (2002) 57–69.
[3] N. Aratani, D. Kim, A. Osuka, Chem. Asian J. 4 (2009) 1172–1182.
[4] N. Aratani, A. Osuka, H.S. Cho, D. Kim, J. Photochem. Photobiol. C 3 (2002) 25–52.
[5] K.S. Kim, J.M. Lim, A. Osuka, D. Kim, J. Photochem. Photobiol. C 9 (2008) 13–28.
[6] K. Zeng, Z. Tong, L. Ma, et al., Energy Environ. Sci. 13 (2020) 1617–1657.
[7] Y. Rio, P. Vázquez, E. Palomares, J. Porphyrins Phthalocyanines 13 (2009) 645–651.
[8] L.L. Li, E.W.G. Diau, Chem. Soc. Rev. 42 (2013) 291–304.
[9] M. Urbani, M. Grätzel, M.K. Nazeeruddin, T. Torres, Chem. Rev. 114 (2014) 12330–12396.
[10] A. Mahmood, J.Y. Hu, B. Xiao, et al., J. Mater. Chem. A 6 (2018) 16769–16797.
[11] Q. Li, C. Li, J. Kim, et al., J. Am. Chem. Soc. 141 (2019) 5294–5302.
[12] J. Yang, M.C. Yoon, H. Yoo, P. Kim, D. Kim, Chem. Soc. Rev. 41 (2012) 4808–4826.
[13] V.S.Y. Lin, S.G. DiMagno, M.J. Therien, Science 264 (1994) 1105–1111.
[14] T. Tanaka, A. Osuka, Chem. Soc. Rev. 44 (2015) 943–969.
[15] Q. Li, C. Li, G. Baryshnikov, et al., Nat. Commun. 11 (2020) 5289.
[16] J. Tian, B. Huang, M.H. Nawaz, W. Zhang, Coord. Chem. Rev. 420 (2020) 213410–213429.
[17] M. Ethirajan, Y. Chen, P. Joshi, R.K. Pandey, Chem. Soc. Rev. 40 (2011) 340–362.
[18] R.D. Teo, J.Y. Hwang, J. Termini, Z. Gross, H.B. Gray, Chem. Rev. 117 (2017) 2711–2729.
[19] M. Rickhaus, A.V. Jentzsch, L. Tejerina, et al., J. Am. Chem. Soc. 139 (2017) 16502–16505.
[20] P.S. Bols, H.L. Anderson, Acc. Chem. Res. 51 (2018) 2083–2092.
[21] O. Wennerström, H. Ericsson, I. Raston, S. Svensson, W. Pimlott, Tetrahedron Lett. 30 (1989) 1129–1132.
[22] J. Song, S.Y. Jang, S. Yamaguchi, et al., Angew. Chem. Int. Ed. 47 (2008) 6004–6007.
[23] J. Song, N. Aratani, J.H. Heo, et al., J. Am. Chem. Soc. 132 (2010) 11868–11869.
[24] C. Maeda, H. Shinokubo, A. Osuka, Org. Lett. 12 (2010) 1820–1823.
[25] Y. Rao, J.O. Kim, W. Kim, et al., Chem. Eur. J. 22 (2016) 8801–8804.
[26] M.O. Senge, M.G.H. Vicente, K.R. Gerzevske, T.P. Forsyth, K.M. Smith, Inorg. Chem. 33 (1994) 5625–5638.
[27] L.J. Esdaile, M.O. Senge, D.P. Arnold, Chem. Commun. (2006) 4192–4194.
[28] L.J. Esdaile, P. Jensen, J.C. McMurtrie, D.P. Arnold, Angew. Chem. Int. Ed. 46 (2007) 2090–2093.
[29] A.M.V.M. Pereira, M.G.P.M.S. Neves, J.A.S. Cavaleiro, et al., Org. Lett. 13 (2011) 4742–4745.
[30] C.H. Devillers, S. Hebié, D. Lucas, et al., J. Org. Chem. 79 (2014) 6424–6434.
[31] A.A. Ryan, S. Plunkett, A. Casey, T. McCabe, M.O. Senge, Chem. Commun. 50 (2014) 353–355.
[32] K. Fujimoto, H. Yorimitsu, A. Osuka, Chem. Eur. J. 21 (2015) 11311–11314.
[33] K. Merahi, A.M.V.M. Pereira, C. Jeandon, et al., J. Porphyrins Phthalocyanines 20 (2016) 1233–1243.
[34] D. Shimizu, K. Fujimoto, A. Osuka, Angew. Chem. Int. Ed. 57 (2018) 9434–9438.
[35] N. Fukui, A. Osuka, Bull. Chem. Soc. Jpn. 91 (2018) 1131–1137.
[36] D. Shimizu, Y. Ide, T. Ikeue, A. Osuka, Angew. Chem. Int. Ed. 58 (2019) 5023–5027.
[37] K. Wang, A. Osuka, J. Song, ACS Cent. Sci. 6 (2020) 2159–2178.
[38] H. Mori, J.M. Lim, D. Kim, A. Osuka, Angew. Chem. Int. Ed. 52 (2013) 12997–13001.
[39] I.M. Blake, L.H. Rees, T.D.W. Claridge, H.L. Anderson, Angew. Chem. Int. Ed. 39 (2000) 1818–1821.
[40] I.M. Blake, A. Krivokapic, M. Katterle, H.L. Anderson, Chem. Commun. (2002) 1662–1663.
[41] L.J. Esdaile, L. Rintoul, M.S. Goh, et al., Chem. Eur. J. 22 (2016) 3430–3446.
[42] Y. Jun-i, N. Fukui, K. Furukawa, A. Osuka, Chem. Eur. J. 24 (2018) 1528–1532.